Available online at www.sciencedirect.com
SCIENCE DIRECT®
Bioorganic & Medicinal Chemistry Letters 15 (2005) 2169–2172
Bioorganic & Medicinal Chemistry Letters

Fluorescence resonance energy transfer studies of aminoglycoside binding to a T box antiterminator RNA

John A. Means and Jennifer V. Hines*

Department of Chemistry and Biochemistry, Ohio University, Athens, OH 45701, USA

Received 3 December 2004; revised 1 February 2005; accepted 2 February 2005
Available online 18 March 2005

Abstract—The T box transcription antitermination mechanism is found in many Gram-positive bacteria. The T box genes are typically tRNA synthetase, amino acid biosynthesis, and amino acid transport genes that have a common transcriptional control mechanism in which a unique RNA–RNA interaction occurs between an uncharged tRNA and the 5′ leader region of the nascent mRNA, leading to antitermination of transcription. The tRNA binds the mRNA in at least two regions: the specifier sequence and the antiterminator. If the latter interaction does not occur, then transcription is terminated. The binding of eight different aminoglycosides to a model of the *Bacillus subtilis tyrS* T box antiterminator RNA has been studied using fluorescence resonance energy transfer. The observed single-site binding dissociation constants were in the low to mid micromolar range. The structure–activity relationship of aminoglycoside binding indicates that selective binding of small molecules to T box antiterminator RNA can be achieved.

The T box transcription antitermination system is present in many amino acid biosynthesis, amino acid transport, and tRNA synthetase genes in Gram-positive bacteria.[1,2] The regulatory system involves a complex set of conserved structural and sequence elements in the 5′ untranslated leader region of the regulated gene mRNA transcript, with the highly conserved T box sequence being located toward the 3′ end of this leader region. Also toward the 3′ end of the mRNA leader region, two mutually exclusive structures can form: the thermodynamically favored terminator and the antiterminator, which incorporates the T box sequence (Fig. 1a).[3] The antiterminator (see Fig. 1b for a model antiterminator RNA) contains two helical domains (A1 and A2) and a highly conserved seven-nucleotide bulge[2] that causes a large kink between the helical domains.[4] To effect antitermination, two different interactions occur between the leader region of the mRNA and the cognate tRNA: the anticodon loop of the cognate tRNA base pairs with the specifier sequence of the leader region, and the 3′ acceptor end of the uncharged cognate tRNA base pairs with the first four bases of the antiterminator bulge (Fig. 1a).[5] This interaction is presumed to preferentially stabilize the antiterminator, thus precluding the formation of the terminator.[3]

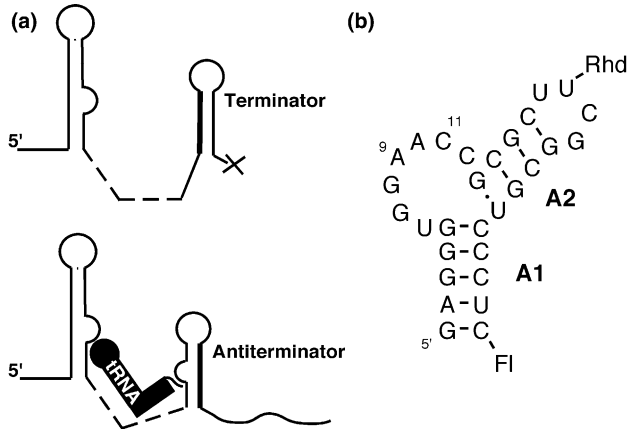

Figure 1. (a) Schematic showing the mutually exclusive terminator and tRNA-stabilized antiterminator structures in the 5′ leader region of the mRNA; (b) structure of antiterminator model RNA 3′-Fl-AM1A-Rhd, illustrating bend that is imposed by the bulge between the two helices—A1 and A2.

Given the unique structure of the antiterminator and the critical role it plays in regulating many important genes in Gram-positive bacteria, it is an intriguing target for

Keywords: Antiterminator RNA aminoglycoside ligand binding.
* Corresponding author. Tel.: +1 740 517 8482; fax: +1 740 593 0148; e-mail: hinesj@ohio.edu

0960-894X/$ - see front matter © 2005 Elsevier Ltd. All rights reserved.
doi:10.1016/j.bmcl.2005.02.007

small molecule ligands. The aminoglycosides are a class of small molecules that are known to bind to various RNAs, including ribosomal RNA;[6] the hammerhead ribozyme;[7] the HDV ribozyme end;[8] group I introns;[9] and the HIV-1 RRE transcriptional activator region.[10] The purpose of this work was to determine whether any aminoglycosides would bind to antiterminator model RNA.

Recently, functionally relevant in vitro RNA models for the antiterminator, including AM1A, were reported.[11] The model bulge sequence is found in other T box genes, and the entire AM1A sequence is functional in the *B. subtilis tyrS* context in vivo.[2] Various fluorescent measurement techniques have been employed to study RNA-small molecule interactions.[12–17] In preliminary studies of the T box antiterminator RNA, a simple fluorescence-quenching assay was employed to measure the binding of the aminoglycosides with a 5′-fluorescein-labeled AM1A antiterminator model. There was no discernable change in the fluorescence spectra of the labeled RNA (data not shown). Since the aminoglycosides are so much smaller than the RNA, the binding of these small molecules with AM1A may not have caused a significant enough conformational change in the RNA to alter the stacking at its 5′ end, which would be needed to induce a change in the fluorescence of the fluorescein. Therefore, fluorescence resonance energy transfer (FRET) was enlisted to measure the aminoglycoside binding with a second, double fluorescently labeled AM1A (Fig. 1b). The nature of the FRET phenomenon (i.e., the distance-dependent transfer of energy from a donor fluorophore to an acceptor fluorophore) potentially would be more sensitive to conformational changes within the antiterminator RNA than would a simple fluorescence-quenching assay. Upon the binding of the aminoglycoside with the AM1A, any slight change in the bend angle or kink between the two helices would potentially be detected by a change in the efficiency of the energy transfer between the donor and acceptor fluorophores.

The aminoglycosides (neomycin B, kanamycin A, kanamycin B, amikacin, tobramycin, paromomycin, gentamicin C, and streptomycin; Fig. 2) were obtained from Sigma, and each was dissolved in ultrapurified water to a concentration of 50 mg/mL and used immediately. The 3′-Fl-AM1A-Rhd model (Fig. 1b) was made by labeling 3′-Fl-18-(2′-amino)-AM1A (Dharmacon) with the *N*-hydroxysuccinimide ester of carboxytetramethylrhodamine using an established procedure.[18] The labeled RNA was dialyzed into 10 mM sodium phosphate pH 6.5, 0.01 mM EDTA prior to use. Binding mixtures consisted of 400 nM 3′-Fl-AM1A-Rhd and a serial dilution of one of the aminoglycosides (range of 0 to 12.5 mg/mL) in 50 mM sodium phosphate pH 6.5, 0.01 mM EDTA, 50 mM NaCl, 5 mM $MgCl_2$. The corresponding background spectra (i.e., reaction mixtures without the labeled RNA) were also obtained. After incubation at 25 °C for 10 min, fluorescence measurements were obtained, using a Molecular Devices FlexStation 96-well plate reader. The 3′-Fl-AM1A-Rhd was excited at 490 nm with a 515 nm cutoff filter, while the emission spectra were obtained for each mixture over the range of 515–640 nm.[19] Fluorescence spectra were obtained at 10, 70, and 130 min.

The intensity data at 585 nm were plotted versus ligand concentration. The fluorescent intensities were corrected for any background fluorescence by the respective aminoglycosides. The normalized relative fluorescent intensities for each experiment were calculated as $F_{rel} = |F - F_0|/F_0$, where F is the fluorescent intensity of the 3′-Fl-AM1A-Rhd, and F_0 is the intensity of the 3′-Fl-AM1A-Rhd with no aminoglycoside present. Using *GraphPad Prism v.4*, replicate data sets for each aminoglycoside were averaged, plotted against the concentration of each aminoglycoside in μM, and analyzed using a one-site binding model. Binding trends were similar at all time points, with data scatter decreasing over time. Representative binding curves for the 130-min data are shown in Figure 3, and binding data are summarized in Table 1. The gentamicin C was supplied as

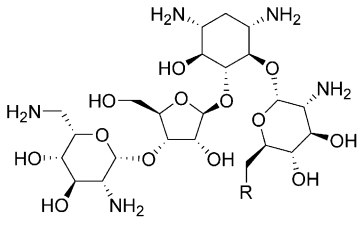

	R
Neomycin B	NH_2
Paromomycin	OH

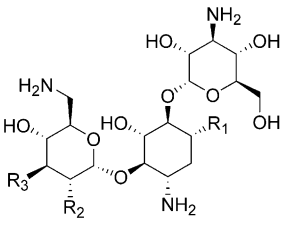

	R_1	R_2	R_3
Tobramycin	NH_2	NH_2	H
Kanamycin B	NH_2	NH_2	OH
Kanamycin A	NH_2	OH	OH
Amikacin	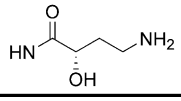	OH	OH

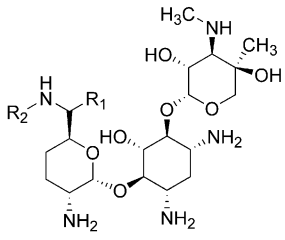

	R_1	R_2
Gentamicin C_1	CH_3	CH_3
Gentamicin C_{1a}	H	H
Gentamicin C_2	H	CH_3

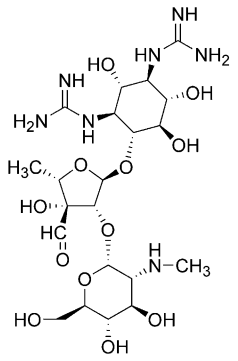

Streptomycin

Figure 2. Structures of aminoglycosides used in study. Aminoglycosides are organized by common core structures (from left to right): 4,5-disubstituted, 4,6-disubstituted, gentamicin C, and streptomycin.

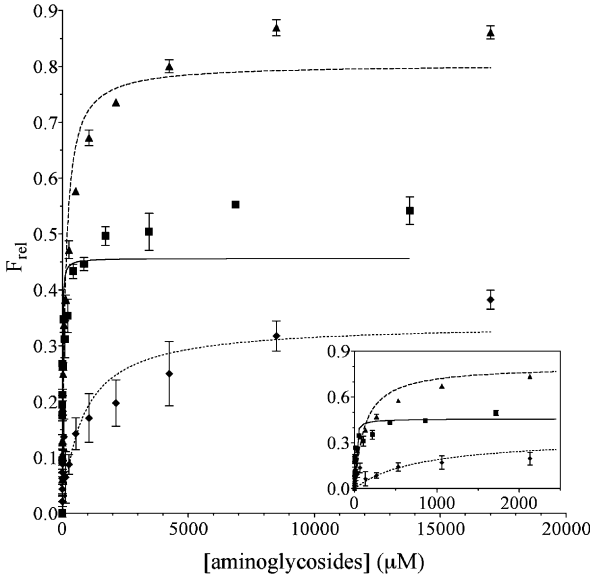

Figure 3. Representative binding curves for aminoglycoside interactions with 3′-Fl-AM1A-Rhd; see text for definition of F_{rel}. The data points and fitted curve, respectively, for neomycin B are the filled square and solid line; for gentamicin C, filled triangles and dashed line; and for streptomycin, filled diamonds and dotted line. (Inset) Rescaling of the data shows the curves at the lower aminoglycoside concentrations. Error bars represent the standard deviation of replicate measurements for each data point.

a mixture of three components. Therefore, for conversion from mg/mL to μM, the molecular weight for gentamicin was calculated as a weighted average of each of the three components, based on information from the vendor.

Of the eight aminoglycosides tested, neomycin had the lowest dissociation constant. This is consistent with previous RNA–aminoglycoside studies where neomycin has typically exhibited the best binding of the monomeric aminoglycosides.[10,20–23] The trend for the dissociation constants of the aminoglycosides tested correlates well with the number of amines. Consequently, the aminoglycosides most likely are interacting with the antiterminator model RNA via, in part, electrostatic interactions, similar to how aminoglycosides bind other RNA motifs.[20,22–24] For paromomycin, gentamicin C, and kanamycin B, the fit to a single-site binding model is very good. In contrast, the fit for kanamycin A and streptomycin is poor. When the data were fit using two-site and higher order binding models, the K_d errors increased substantially, indicating that none of these alternate models entirely explain the data. In addition, when the fits for single-site (hyperbolic) binding versus nonspecific (linear) binding were compared, the single-site binding was better as determined by the F-test ($P = 0.05$). One possible explanation for these fit observations is that there is a mixture of specific and non-specific binding. Another possibility is that the observed binding curve may be an average of multiple-site binding in fast exchange. Finally, it is also possible that there may be aminoglycoside binding modes that do not directly result in a significant change in the FRET and are, therefore, silent in this assay.

Table 1. Single-site binding data for aminoglycoside binding with 3′-Fl-AM1A-Rhd

Aminoglycosides	No. of amines	K_d (μM)[a]	Max. F_{rel}[b]
Neomycin B	6	8.5 ± 2.1 (0.82)	0.46 ± 0.02
Tobramycin	5	38 ± 9.0 (0.89)	0.33 ± 0.01
Paromomycin	5	50 ± 9.4 (0.92)	0.41 ± 0.01
Gentamicin C	5	120 ± 19 (0.95)	0.80 ± 0.03
Kanamycin B	5	150 ± 27 (0.94)	0.38 ± 0.01
Kanamycin A	4	210 ± 87 (0.67)	0.21 ± 0.02
Amikacin	4	760 ± 270 (0.73)	0.29 ± 0.03
Streptomycin	1	790 ± 310 (0.68)	0.34 ± 0.03

[a] Goodness-of-fit values (R^2) in parentheses.
[b] See text for definition of F_{rel}.

Another observation from the data is that the maximal F_{rel} values (Table 1) are similar for each of the aminoglycoside molecules within a common core structure set, and the maximal F_{rel} varies between different core structure sets (see Fig. 2 for groupings). Since the F_{rel} ultimately reflects the ligand-induced change in the distance between the donor and acceptor fluorophores, this correlation strongly suggests a structure-specific conformational change in the RNA upon binding of each of the related groups of aminoglycosides. The maximal F_{rel} of the 4,5-disubstituted derivatives (neomycin B, paromomycin) is between 0.41 and 0.46, while that of the 4,6-disubstituted derivatives (tobramycin, kanamycin B, kanamycin A, amikacin) is between 0.21 and 0.38. Even though the basic structure of gentamicin C ($F_{rel} = 0.80$) is similar to the structure of the latter grouping, it is more hydrophobic; therefore, it would not necessarily affect the RNA conformation in the same manner. Similar core structure–activity relationships have been seen in other fluorescent RNA–aminoglycoside binding studies.[22]

In addition to the maximal F_{rel} trends discussed above, the corrected rhodamine fluorescent intensities decreased as the aminoglycoside concentrations increased. This implies that the antiterminator RNA structure is undergoing a conformational change that results in a less efficient transfer of energy between the fluorescent moieties upon the binding of an aminoglycoside. One possibility would be an alteration of the bend angle between helix A1 and helix A2, resulting in a change in distance/orientation between the donor–acceptor pair. Previous structural studies of AM1A indicated a bend angle of 56°, where the kink was induced by extensive base stacking at the 3′ end of the seven-nucleotide bulge.[4] Any change in the structure of the bulge nucleotides (e.g., due to aminoglycoside binding) would most likely affect the bend angle between the two helices. In an alternative antiterminator model RNA, where a single fluorescent label (2-aminopurine)[13,25,26] is introduced in the bulge at position 9, fluorescence quenching occurs upon addition of the aminoglycosides, consistent with the interpretation that the aminoglycosides are binding in the region of the bulge nucleotides (J. Means, J. Hines, unpublished results).

Extensive research with other RNA motifs, including small bulges (TAR)[27] and internal loops (RRE)[28] have shown that aminoglycosides bind readily to bulged bases and RNA pockets, especially divalent metal ion binding sites. The 93-fold selectivity difference between the tightest-binding aminoglycoside (neomycin B) and the weakest (streptomycin), as well as the four-fold selectivity difference between tobramycin and kanamycin B (each containing five amines), indicate that the antiterminator RNA is most likely forming a unique RNA pocket amenable to selective, small molecule binding. This pocket may also be a divalent metal ion binding site. This notion is consistent with UV thermal denaturation studies that show a saturable magnesium-specific binding trend in T_m melting temperatures (K. Jack and J. Hines, unpublished results).

In this paper, fluorescence resonance energy transfer spectroscopy was used to study the binding of aminoglycosides with a model of the T box antiterminator RNA. This is the first literature example of small ligands specifically binding the biologically significant regulatory T box antiterminator RNA. Further studies are on-going to determine the exact aminoglycoside binding mode and location within the antiterminator, as well as to utilize the aminoglycoside binding data for targeted ligand design with the ultimate goal of disruption of the tRNA–antiterminator complex.

Acknowledgements

This work was supported by NIH grant RO1-GM61048, Battelle Memorial Institute (SOSCI Project), and the Office of the Vice President for Research, Ohio University.

References and notes

1. Grundy, F. J.; Henkin, T. M. *Cell* **1993**, *74*, 475.
2. Grundy, F. J.; Moir, T. R.; Haldeman, M. T.; Henkin, T. M. *Nucl. Acids Res.* **2002**, *30*, 1646.
3. Henkin, T. M. *Mol. Microbiol.* **1994**, *13*, 381.
4. Gerdeman, M. S.; Henkin, T. M.; Hines, J. V. *J. Mol. Biol.* **2003**, *326*, 189.
5. Grundy, F. J.; Collins, J. A.; Rollins, S. M.; Henkin, T. M. *RNA* **2000**, *6*, 1131.
6. Fourmy, D.; Recht, M. I.; Puglisi, J. D. *J. Mol. Biol.* **1998**, *277*, 347.
7. Stage, T. K.; Hertel, K. J.; Uhlenbeck, O. C. *RNA* **1995**, *1*, 95.
8. Chia, J. S.; Wu, H. L.; Wang, H. W.; Chen, D. S.; Chen, P. J. *J. Biomed. Sci.* **1997**, *4*, 208.
9. Hoch, I.; Berens, C.; Westhof, E.; Schroeder, R. *J. Mol. Biol.* **1998**, *282*, 557.
10. Zapp, M. L.; Stern, S.; Green, M. R. *Cell* **1993**, *74*, 969.
11. Gerdeman, M. S.; Henkin, T. M.; Hines, J. V. *Nucl. Acids Res.* **2002**, *30*, 1065.
12. Klostermeier, D.; Sears, P.; Wong, C. H.; Millar, D. P.; Williamson, J. R. *Nucl. Acids Res.* **2004**, *32*, 2707.
13. Bradrick, T. D.; Marino, J. P. *RNA* **2004**, *10*, 1459.
14. Gayle, A. Y.; Baranger, A. M. *Bioorg. Med. Chem. Lett.* **2002**, *12*, 2839.
15. Lacourciere, K. A.; Stivers, J. T.; Marino, J. P. *Biochemistry* **2000**, *39*, 5630.
16. Llano-Sotelo, B.; Chow, C. S. *Bioorg. Med. Chem. Lett.* **1999**, *9*, 213.
17. Wang, Y.; Hamasaki, K.; Rando, R. R. *Biochemistry* **1997**, *36*, 768.
18. Walter, N. G. In *Current Protocols in Nucleic Acid Chemistry*; Beaucage, S. L., Bergstrom, D. E., Glick, G. D., Jones, R. A., Eds.; John Wiley and Sons: New York, 2002; pp 11.10.11–11.10.23.
19. Clegg, R. M. *Methods Enzymol.* **1992**, *211*, 353.
20. Wong, C. H.; Hendrix, M.; Priestley, E. S.; Greenberg, W. A. *Chem. Biol.* **1998**, *5*, 397.
21. Kirk, S. R.; Tor, Y. *Bioorg. Med. Chem.* **1999**, *7*, 1979.
22. Blount, K. F.; Tor, Y. *Nucl. Acids Res.* **2003**, *31*, 5490.
23. Mikkelsen, N. E.; Brannvall, M.; Virtanen, A.; Kirsebom, L. A. *Proc. Natl. Acad. Sci. U.S.A.* **1999**, *96*, 6155.
24. Hendrix, M.; Priestley, E. S.; Joyce, G. F.; Wong, C. H. *J. Am. Chem. Soc.* **1997**, *119*, 3641.
25. Harris, D. A.; Rueda, D.; Walter, N. G. *Biochemistry* **2002**, *41*, 12051.
26. Zagorowska, I.; Adamiak, R. W. *Biochimie* **1996**, *78*, 123.
27. Faber, C.; Sticht, H.; Schweimer, K.; Rosch, P. *J. Biol. Chem.* **2000**, *275*, 20660.
28. McPike, M. P.; Goodisman, J.; Dabrowiak, J. C. *Bioorg. Med. Chem.* **2004**, *12*, 1835.